

# Adsorption of $\text{Cu}^{2+}$ and $\text{Ni}^{2+}$ on iron oxide and kaolin and its importance on $\text{Ni}^{2+}$ transport in porous media

Tushar Kanti Sen<sup>1</sup>, S.P. Mahajan, Kartic C. Khilar\*

*Department of Chemical Engineering, Indian Institute of Technology, Bombay Powai, Mumbai-400076, India*

---

## Abstract

Adsorption of divalent heavy metal ions on iron oxide and kaolin is important to determine the transport and ultimate fate of ions in underground water and soil. In this study, kinetics and equilibrium adsorption of  $\text{Cu}^{2+}$  and  $\text{Ni}^{2+}$  metal ions from their aqueous solutions on iron oxide, kaolin and sand have been investigated. Batch adsorption studies show that  $\text{Cu}^{2+}$  and  $\text{Ni}^{2+}$  adsorb more strongly on the colloidal fines, iron oxide and kaolin than on the sand material. It is shown that the adsorption of  $\text{Cu}^{2+}$  and  $\text{Ni}^{2+}$  is a function of system pH, and solid adsorbent concentration. The equilibrium data follow the most widely used nonlinear Freundlich isotherm equilibrium model which has the general form of  $X = K_F C^n$ . It is found that 'n' is strongly dependent on the nature of the adsorbent and virtually independent of conditions such as pH. The other parameter, ' $K_F$ ' strongly depends on the pH of the solution. Finally, predictions of contaminant transport of  $\text{Ni}^{2+}$  due to the presence of colloidal fines, kaolin based on batch adsorption value has been compared with measured data using sand-kaolin packed beds.

*Keywords:* Freundlich isotherm; Oxide particles; Metal adsorption; Kinetics; Colloid-associated transport

---

## 1. Introduction

The fate and transport of metal ions in ground-water as well as in water treatment processes are often controlled by sorption with soil and soil fines. Field investigations have shown that small colloidal particles or fines that are ubiquitous in the natural environment, are mostly composed of

hydrous oxides of Al, Fe, Mn and aluminosilicates such as clays. Experimental as well as theoretical studies have also found that these mobile colloidal fines can often carry contaminants such as radionuclides, transition metals and hydrophobic organics adsorbed onto their surface and can, thus, significantly accelerate the transport of contaminants through porous media [1–6]. Infact, strong adsorption/association of contaminants on colloidal fines is a necessary condition in colloid-associated contaminant transport in porous media. Cationic forms of the metals (cation) are the most frequently reported contaminants influenced by this colloid-associated transport.

---

\* Corresponding author

E-mail address: [kartic@cupid.che.iitb.ac.in](mailto:kartic@cupid.che.iitb.ac.in) (K.C. Khilar).

<sup>1</sup> Present address: Department of Chemical Engineering, Regional Engineering College, Rourkela-769008, Orissa, India.  
E-mail:

[tksen@nitrkl.ac.in](mailto:tksen@nitrkl.ac.in)

Large number of experimental and modeling studies have been reported on the adsorption of cations, particularly heavy metal ions on to pure soil components such as clay minerals, and oxides at different values of pH, metal ion, solid/liquid ratio and temperature and only few references are mentioned herewith [7–19]. These studies, in general show that the adsorption of cations is favored at higher pH and the maximum enhancement in adsorption occurs over a narrow region of 1–2-pH units. Langmuir adsorption isotherms as well as Freundlich adsorption isotherms have been used to describe the equilibrium. Subramaniam et al. [15] have shown that copper adsorption on to ferric oxide and on to silicon particles increases with an increase in pH but there is a very weak effect on the adsorption due to the changes in concentration of added electrolyte. Benjamin and Leckie [13] developed a heterogeneous site model for the surface of iron oxide, which can successfully explain the adsorption of Cd, Zn, Cu and Pb as a function of pH, metal ion concentration and adsorbent concentration. Angove et al. [9] studied the adsorption  $\text{Cd}^{2+}$  and  $\text{Co}^{2+}$  on to kaolin. They have shown that two different mechanisms of adsorption operate depending on the pH. At low pH the metal ions adsorb only by ion exchange at relatively sparse permanently charged sites on the siloxanol faces. At higher pH,  $\text{Cd}^{2+}$  and  $\text{Co}^{2+}$  adsorb to more closely spaced variable charge (probably aluminol) groups at the crystal edges, with the formation of inner sphere complexes. Surface complexation models (SCMs) have been shown to be capable of describing metal ions adsorption onto mineral surfaces [11,18,19,21]. All these studies have been carried out with higher metal ion concentration ranges.

In this study, we present a new data set on adsorption of  $\text{Ni}^{2+}$  and  $\text{Cu}^{2+}$  to pure soil components as influenced by pH, initial total metal ion concentrations and adsorbent concentration within the groundwater metal ion concentration ranges which are useful to predict the transport behavior of colloid-associated metal ions in porous media. Batch adsorption studies show that there are substantial amounts of adsorption of contaminants  $\text{Cu}^{2+}$ ,  $\text{Ni}^{2+}$  on colloidal fines, kaolin and iron oxide. The adsorption on to

sand material is found to be comparatively low, primarily due to the significantly less exposed surface area. It is also found that Freundlich isotherm ( $X = K_F C^j$ ) is appropriate for describing adsorption characteristics of  $\text{Ni}^{2+}$  and  $\text{Cu}^{2+}$  with kaolin, iron oxide and sand material.

The transport of  $\text{Ni}^{2+}$  ions through sand–kaolin packed beds are predicted by using data from adsorption experiments and a suitable mathematical model. Predictions of transport of  $\text{Ni}^{2+}$  due to the presence of colloidal fines, kaolin using equilibrium adsorption parameters as obtained from batch adsorption have been compared with the experimental measurements of flow and transport in sand–kaolin beds. It is shown that the adsorption in the column is over predicted implying a limited use of batch adsorption values in the analysis of contaminant transport.

## 2. Experimental studies

### 2.1. Materials and methods

All chemicals used were of analytical grade. Salts used in the preparation of synthetic contaminant bearing solutions are  $\text{Ni}(\text{NO}_3)_2 \cdot 6\text{H}_2\text{O}$ , and  $\text{CuCl}_2 \cdot 2\text{H}_2\text{O}$ , obtained from S.D. fine chemicals, Mumbai, India. The pH of the system was adjusted using reagent grade aqueous ammonia solution (diluted from 30% solution) for higher alkali range to avoid precipitation with NaOH solution. Aqueous solution of corresponding metal salts was in the mild acidic range ( $4.5 \pm 0.1$ ). Kaolin (BET surface area =  $33.50 \text{ m}^2\text{g}^{-1}$ , Sauter mean diameter =  $2.80 \text{ }\mu\text{m}$ ) was obtained from Sastick Chemicals, Mumbai. Crystalline iron oxide of 30 mesh size was obtained from Aldrich and then was crushed in a centrifugal ball mill to obtain a powder (BET surface area =  $191.6 \text{ m}^2\text{g}^{-1}$ , Sauter mean diameter =  $3.0 \text{ }\mu\text{m}$ ). This was used as such after drying at a temperature of  $70 \text{ }^\circ\text{C}$  in a temperature-controlled oven. The ENNORE sand used in both batch and column studies, obtained from Tamil Nadu Minerals Ltd., India and it is quartz of light gray or whitish variety and free from slit. The sieve fraction was such that it was retained by  $0.693 \text{ mm}$  sieve and

passed through 0.853 mm openings. The sand prior to its use in batch as well as column experiments, was cleaned as per the procedures used by Johnson et al. [20] and oven dried at 105 °C for 24 h. Double distilled water was used for cleaning of sand as well as for all experimental purposes. All plastic sample bottles and glassware were cleaned, then rinsed with double distilled water and dried at 60 °C in a temperature-controlled oven. All measurements were conducted at the room temperature ( $28 \pm 2$  °C).

The concentrations of  $\text{Cu}^{2+}$  and  $\text{Ni}^{2+}$  were measured using GBC double beam flame atomic absorption spectrophotometer, GBC scientific Equipment Pvt. Ltd., Australia. Sizes of colloidal particles were measured by Master Sizer X Ver.1.2, Malvern Instruments Ltd., UK. The pH was measured using a control Dynamics pH meter, India.

## 2.2. Experimental procedures for adsorption studies

The metal ions uptake from aqueous solutions by colloidal fines as well as by sand was measured by placing 30 ml of ion solution into contact with 8 mg of colloidal fines in series of 60 ml plastic bottles. This amount of solid/liquid ratio is within the range of the underground colloidal fines concentration. Initial total metal ion concentration range was 8–30  $\text{mg l}^{-1}$ , comparable with the concentration range of contaminants in groundwater. For metal–sand system, solid/liquid ratio was 6 g 30  $\text{ml}^{-1}$  in a series of stopper bottles. Samples were shaken on a temperature controlled rotary shaker and the speed was such that it maintains the contents completely mixed and the colloidal particles were suspended throughout the vessel. A period of 6 h was found to be sufficient to attain equilibrium. The solutions pH was adjusted before starting the sorption experiments. After equilibrium time, the contents were filtered through a Whatman glass micro filter (0.2  $\mu\text{m}$  size) and then analyzed for  $\text{Cu}^{2+}$  and  $\text{Ni}^{2+}$  ions. The concentration of the metal ions in solutions and the medium pH were determined both before and after adsorption experiments by flame atomic absorption spectrophotometer and with a pH meter, respectively. The quantity of adsorbed

metal ion on iron oxide and kaolin as well as sand was calculated as the difference between initial concentration and concentration at equilibrium. Each experiment was repeated in twice to check the reproducibility. Measurements are, in general, reproducible within  $\pm 10\%$ .

The kinetics of adsorption of  $\text{Ni}^{2+}$  and  $\text{Cu}^{2+}$  were studied at low and high initial total metal ion concentration (between 12 and 23.6  $\text{mg l}^{-1}$ ) and at different pH on colloidal fines as well as on sand using experimental procedures similar to used in equilibrium studies. The only difference was that samples were collected and analyzed at regular intervals during adsorption process.

## 2.3. Transport experiments

Contaminant transport experiments were conducted using an experimental set-up, consists of a 0.305 m long and 2.5 cm inner diameter acrylic column. Both the ends of column are connected with circular threaded caps. The column is fitted with 60  $\mu\text{m}$  wire mesh supported on a perforated distributor at both ends.

Either distilled water or aqueous solution of  $\text{Ni}^{2+}$  was injected into the sand and sand–kaolin packed column at a fixed flow rate by a variable speed peristaltic pump (Electro lab, Mumbai, India, range 0.5–120  $\text{ml min}^{-1}$ ), which was placed at the bottom of the vertical column. Experiments were conducted with sand size/kaolin size ratio, (SR) of 277. The SR is calculated as the ratio of sauter mean size of sand to the sauter mean size of kaolin particles. For each set of experiments, fresh column was packed to a height of 0.279 m by pouring clean and dried sand of particle density 2666  $\text{kg m}^{-3}$  or sand containing different weight percentage of kaolin. The sand or sand–kaolin mixture of said amount was poured in 2 cm increments into column, which was prefilled with double distilled water (100–110 ml) and stirred to prevent air entrapment. Basically this wet-packing method succeeded in excluding air from the column. U-tube glass manometer were used to measure the pressure drop across the bed.

Initially approximately 15–20 pore volumes (PVs) of double distilled water was sent through the packed column at the chosen flow rate till

turbidity of the effluent was found to be almost nil to remove particles suspended in the bed and to stabilize the system. The effluent from the column was collected at fixed time intervals for measuring  $\text{Ni}^{2+}$  concentration as well as for kaolin particle concentration.

### 3. Results and discussions

#### 3.1. Equilibrium time and capacity

Typical plots showing the kinetics of adsorption of  $\text{Cu}^{2+}$  and  $\text{Ni}^{2+}$  at different initial total metal ion concentrations (low to high) on iron oxide, kaolin, and on sand at different pH are presented in Figs. 1 and 2. Fig. 1(a) shows the result of amounts of adsorption with time for Cu–iron oxide system at a total copper ion concentrations of 13.4 and 23.6  $\text{mg l}^{-1}$ , respectively, at a pH of 4.5 and 6.8, respectively. Similarly, Fig. 1(b) presents the results for Cu–kaolin system at two different concentrations as well as two different pHs. Fig. 2(a) presents the results on kinetics of adsorption of  $\text{Ni}^{2+}$  on iron oxide particles. Fig. 2(b) presents the plots between amount of adsorption and time for metal ion-sand system. From these plots, it is found that the adsorption density i.e. mg of adsorbate per gram of adsorbent increases with increasing contact time and equilibrium is attained within 4 h. These preliminary kinetic experiments strongly indicate that the adsorption of  $\text{Ni}^{2+}$  and  $\text{Cu}^{2+}$  metal ions on oxides is a two-step process: a rapid adsorption of metal ions to the external surface is followed by possible slow intraparticle diffusion in the interior of the particles. In case of kaolin, intraparticle diffusion occurs through the space between the lattice layers, while in case of iron oxide, intraparticle diffusion occurs in the micropores of the oxide particles. This two-stage metal uptake can also be explained as adsorption occurring onto two different types of binding sites on the adsorbent particles. Similar of results have also been obtained by other investigators [7,13,15,18].

To measure the capacity, adsorption experiments were carried out with the wide ranges of initial total metal ion concentration of 10–800 mg

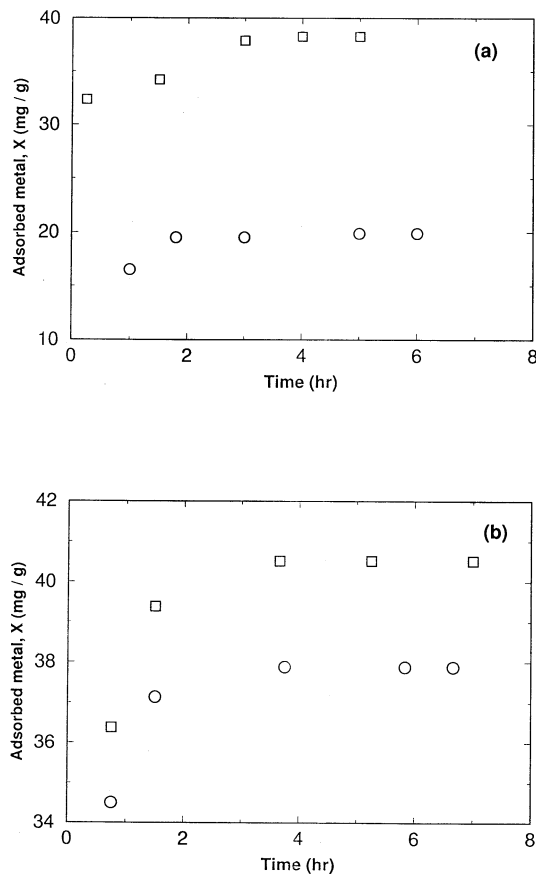


Fig. 1. Kinetics of adsorption. (a) Cu–iron oxide system, ○ Initial  $\text{Cu}^{2+}$ , 13.4  $\text{mg l}^{-1}$ ; pH, 6.8; □ Initial  $\text{Cu}^{2+}$ , 23.6  $\text{mg l}^{-1}$ ; pH, 4.5; (b) Cu–kaolin system, ○ Initial  $\text{Cu}^{2+}$ , 12.00  $\text{mg l}^{-1}$ ; pH, 10; □ Initial  $\text{Cu}^{2+}$ , 23.6  $\text{mg l}^{-1}$ ; pH 4.5.

$\text{l}^{-1}$  and a solid/liquid ratio of 8 mg 30  $\text{ml}^{-1}$  at room temperature and at pH of 4.5. It has been found from Fig. 3(a) and 3(b) that the amount of adsorption increases with increasing total metal ion concentration and attains a maximum value. One observes from Fig. 3(a) that the adsorption capacity of kaolin and iron oxide for  $\text{Ni}^{2+}$  is between 400 and 500  $\text{mg g}^{-1}$  and from Fig. 3(b), that the adsorption capacity for  $\text{Cu}^{2+}$  is between 150 and 250  $\text{mg g}^{-1}$  with iron oxide having higher adsorption capacity. Higher adsorption for  $\text{Ni}^{2+}$  as compared with that of  $\text{Cu}^{2+}$  can be attributed to the relatively smaller size of the  $\text{Ni}^{2+}$  ions as well as to the difference in amounts of surface charge generated. Iron oxide being a better ad-

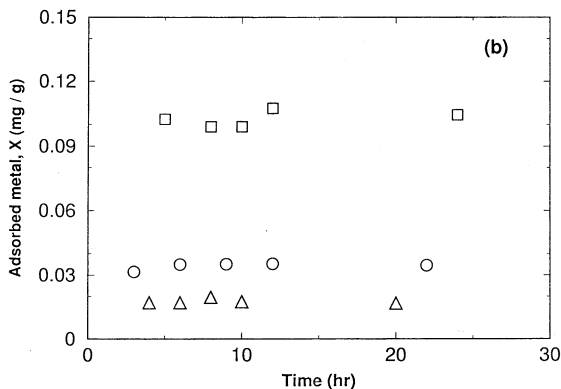
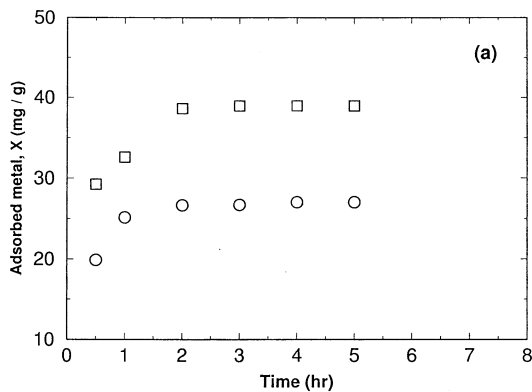


Fig. 2. Kinetics of adsorption. (a) Ni-iron oxide system, ○ Initial  $\text{Ni}^{2+}$ ,  $21.7 \text{ mg l}^{-1}$ ; pH, 4.5; □ Initial  $\text{Ni}^{2+}$ ,  $14.00 \text{ mg l}^{-1}$ ; pH, 7.4. (b) Cu-sand, ○ Initial  $\text{Cu}^{2+}$ ,  $12.3 \text{ mg l}^{-1}$ ; pH, 4.5; □ Ni-sand, Initial  $\text{Ni}^{2+}$ ,  $22.7 \text{ mg l}^{-1}$ ; pH, 11.5 and △ Ni-sand, Initial  $\text{Ni}^{2+}$ ,  $22.7 \text{ mg l}^{-1}$ ; pH, 4.5.

sorbent can be partly attributed to the occurrence of specific adsorption on iron oxide. Specific adsorption which, is due to both the electrostatic as well as chemical forces of attraction, generally gives higher amount of adsorption.

### 3.2. Effect of solid adsorbent concentration

Table 1 presents the effects of solid adsorbent concentration on Freundlich adsorption characteristics parameter for Ni-colloidal fines and Cu-colloidal fines systems, respectively. The solid concentrations are within the colloidal fines concentration range found in underground environ-

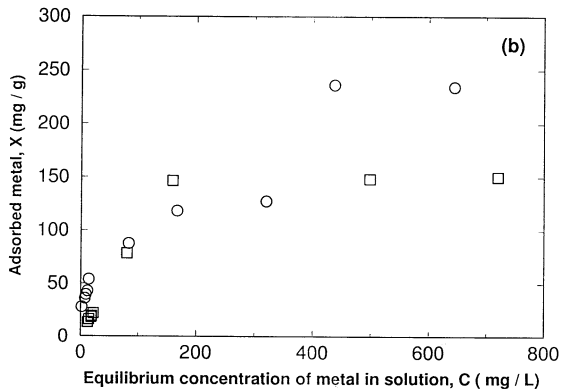
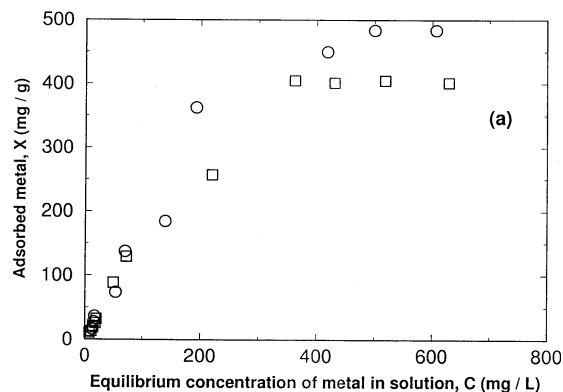


Fig. 3. Maximum adsorption capacity isotherms. (a) ○ Ni-iron oxide; □ Ni-kaolin system; Equilibrium time, 7 h; pH, 4.5; (b) ○ Cu-iron oxide; □ Cu-kaolin; Equilibrium time, 7 h; pH, 4.5.

ment. Typical isotherm plots which are presented elsewhere [33] as amount of metal adsorption per unit mass of adsorbent,  $X \text{ (mg g}^{-1}\text{)}$  against equilibrium aqueous phase concentration of adsorbate metal ion,  $C \text{ (mg l}^{-1}\text{)}$ . Plots are fitted with Freundlich isotherm equation with linear regression coefficient of above 90%.

For Ni-iron oxide and Ni-kaolin systems adsorbent concentrations range was 50, 133.33 and  $266.66 \text{ mg l}^{-1}$ , respectively, whereas, for Cu-iron oxide and for Cu-kaolin system it was 50 and  $266.66 \text{ mg l}^{-1}$ , respectively. From Table 1 one can observe that Freundlich adsorption characteristic parameter particularly adsorbent capacity, ' $K_F$ ', apart from intensity of adsorption, ' $n$ ' declines as the mass of available adsorbent per unit volume

Table 1

Effect of solid adsorbent concentration on Freundlich adsorption characteristics parameters,  $X = K_F C^n$ 

System	Solid conc. (mg l <sup>-1</sup> )	pH	$K_F$ (l g <sup>-1</sup> )	$n$	Initial metal ion concentration (mg l <sup>-1</sup> )
Ni–iron oxide	50.00	4.5	36.30	0.394	17.1, 19.3, 22.8 and 26.4
	133.33	4.5	16.59	0.277	
	266.66	4.5	5.00	0.57	
Ni–kaolin	50.00	4.5	2.87	1.18	18.1, 19.9, 22.7, 23.8 and 26.3
	133.33	4.5	2.00	0.72	
	266.66	4.5	1.72	0.95	
Cu–iron oxide	50.00	4.5	25.11	0.625	12.2, 16.1 17.9, 22.4 and 27.0
	266.33	4.5	19.05	0.287	
Cu–kaolin	50.00	4.5	3.45	1.18	16.2, 19.2, 23.7, 25.1 and 28.5
	266.33	4.5	1.92	0.77	

increases for fixed initial total metal ion concentrations and pH.

Several other investigators have also reported the same trend of particle concentration effect on adsorption [22–28]. Investigators have offered different explanations for the observed dependency. These explanations can be categorized into two groups: (1) ‘real’ physical/chemical processes, and (2) experimental artifacts. One rationalization offered in the ‘real’ category is that the particle concentration effect is thought to be caused by particle–particle interactions. In systems with higher solids content, these interactions are perhaps physically blocking some adsorption sites from the adsorbing solutes and, thus, causing decreased adsorption, or creating electrostatic interferences such that the electrical surface charges on the closely packed particles diminish attractions between the adsorbing solutes and surfaces of individual grains. In terms of physical effects, individual particles in a slurry having a high solid-to-solution ratio may have a greater tendency to coagulate and flocculate into larger particles that have less available surface adsorption sites than individual grains and, thus, can adsorb less adsorbate.

Plausible experimental artifacts include less efficient separation of the solid phase from high solids-content slurries, such that more colloidal size particles laden with adsorbate remain in the solution phase and the associated adsorbate gets included in the analysis of the solution phase. An additional complexing or sorbing agent may be

originally associated with the particles which appears to be dissolved. It is not removed by the particle separation technique but actually complexes (if it is a ligand such as dissolved organic carbon) or sorbs (if it is a colloidal particles) some dissolved chemical. If it is assumed that the concentration of the third phase increases with the concentration of added particles, then infact an apparent reduction in adsorption is consistent with increasing particle concentration since the experimentally determined ‘dissolved’ concentration is actually the sum of the truly dissolved and the additional sorbed or complexed chemical. This is applicable for those adsorbents such as clays, sediments etc in their natural environments, as those may adsorb various organic/inorganic substances to which they are exposed.

The explanations for the particle concentration (solid-to-solution ratio) effect are many and rather perplexing. The origin of this effect, as we believe, depends on the system, particularly the nature of adsorbent. Further studies are required to obtain a complete understanding of this effect. In our study, we have kept the solid loading the same for all our experiments.

### 3.3. Adsorption equilibrium studies

Typical adsorption isotherms for Cu<sup>2+</sup> metal ion on iron oxide and kaolin are presented in Fig. 4 and that for Ni<sup>2+</sup> metal ion on iron oxide and on kaolin are presented in Fig. 5, respectively. Figs. 4 and 5, show the relationship between the concen-

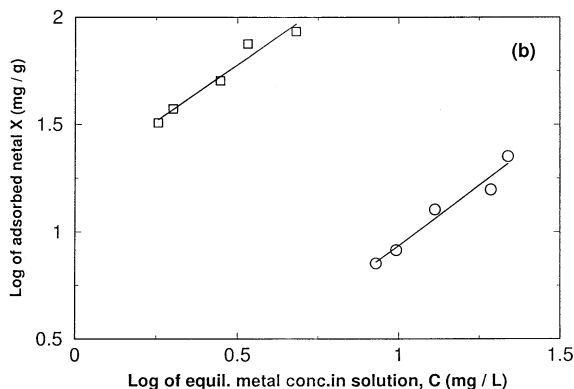
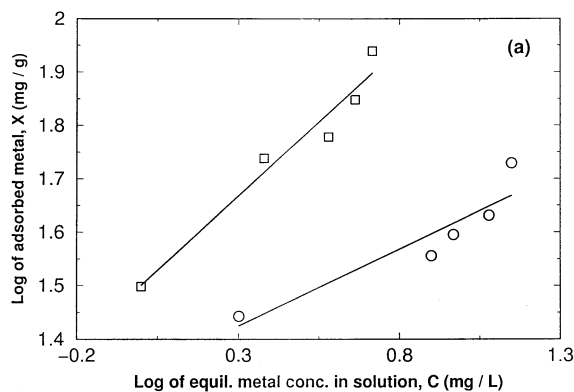


Fig. 4. Effect of pH on Freundlich adsorption isotherm. (a)  $\circ$  pH, 4.5; Coeff., 0.92;  $\square$  pH, 11.5; Coeff., 0.97; Cu-iron oxide system, (b)  $\circ$  pH, 4.5; Coeff., 0.97;  $\square$  pH, 11.5; Coeff., 0.97; Cu-kaolin system.

trations of metal ions adsorbed per unit mass of adsorbent ( $X = \text{mg g}^{-1}$ ), with the concentration of metal ion in solution at equilibrium. These sorption experiments were carried out within a small metal ion concentration range based on groundwater contaminant concentration range i. e.  $10\text{--}30 \text{ mg l}^{-1}$  and with a solid/liquid ratio of  $8 \text{ mg } 30 \text{ ml}^{-1}$ . Within this small concentration range, Freundlich model is found to be satisfactory for describing the equilibrium relationships. Freundlich equation is given as  $X = K_F C^n$ , where  $K_F$  is the empirical distribution parameter and it gives a measure of adsorbent capacity,  $X$  is the adsorbed metal ions on colloidal fines ( $\text{mg g}^{-1}$ ),  $C$  is the metal ion solution equilibrium concentration ( $\text{mg l}^{-1}$ ) and  $n$  is an empirical exponent parameter

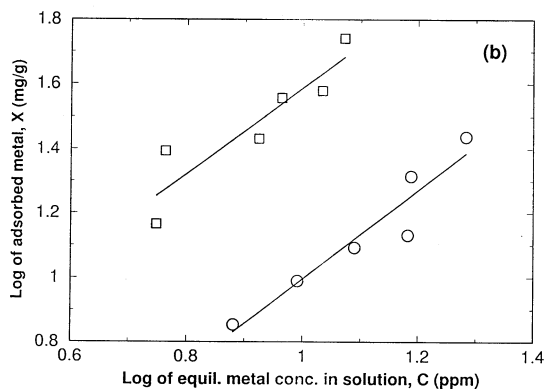
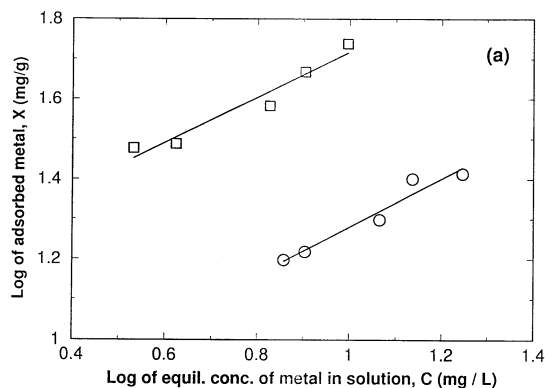


Fig. 5. Effect of pH on Freundlich adsorption isotherm. (a)  $\circ$  pH, 4.5; Coeff., 0.97;  $\square$  pH, 11.5; Coeff., 0.97; Ni-iron oxide system, (b)  $\circ$  pH, 4.5; Coeff., 0.95;  $\square$  pH, 11.5; Coeff., 0.91; Ni-kaolin system.

which gives the intensity of adsorption. For determination of these coefficients, data are usually fitted to the logarithmic form of equation,  $X = K_F C^n$ . Adsorption equilibrium has been approximated with linear regression coefficient of above 90% (solid line in plots) by a single Freundlich isotherm. Although Freundlich equation has been fitted for most of the isotherms, for Cu-iron oxide system as can be seen from Fig. 4(a), the data, however, cannot be best described by a single Freundlich equation for the entire range. It can be fitted with two Freundlich equations (Fig. 6) with different slopes (i.e. two different intensity of adsorption), indicating the existence of two different sets of adsorption sites with substantial difference in energy of adsorption.

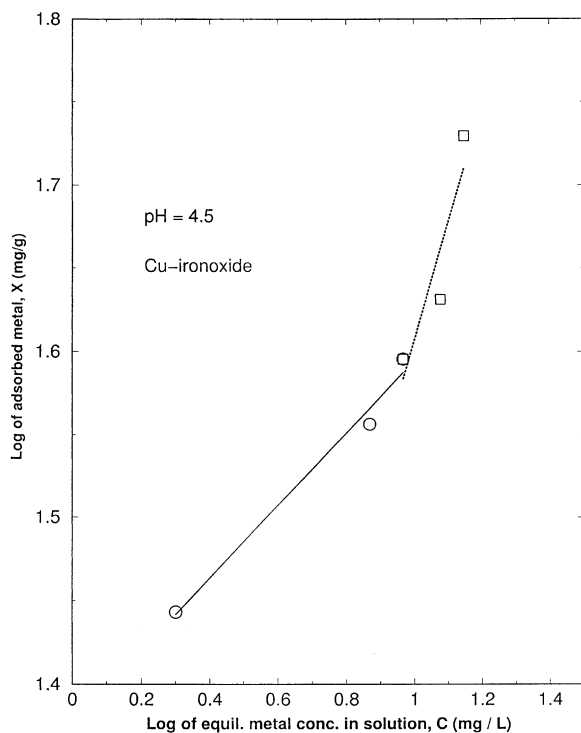


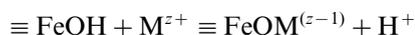
Fig. 6. Double fitted Freundlich adsorption isotherms for Cu-iron oxide system. — ○ 'n', 0.217; ' $K_F$ ', 23.44, Coeff., 0.99, ... □ 'n', 0.70; ' $K_F$ ', 7.94; Coeff., 0.92; pH, 4.5.

### 3.3.1. Effect of pH

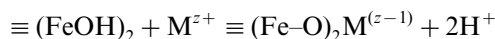
From the adsorption isotherms (Figs. 4 and 5), it has been found that for all systems, amount of adsorption of metal cations,  $Ni^{2+}$  and  $Cu^{2+}$  increases with increase in pH or alkalinity. Such increase in adsorption can be attributed to the favorable change in surface charge and to the extent of hydrolysis of the adsorbing metal ion change with varying pH. As the surface charge becomes more negative with increasing pH, the surface attracts bivalent metal cations for adsorption. Furthermore, the proportion of hydrated ions increases with pH and these may be more strongly adsorbed than unhydrated ions. Therefore, both these effects are synergistically enhancing the amount of adsorption at higher pH.

Specific adsorption is believed to occur as well for iron oxide. This adsorption involves interaction with deprotonated surface hydroxyl groups to

form mono and binuclear inner sphere complexes i.e.



and



Cation adsorption is accompanied by release of protons. The number of protons released per cation adsorbed is termed as  $z$ .

The adsorption on kaolin surface is qualitatively different than that on iron oxide. Two types of binding sites on kaolin are available: weakly acidic group, which undergo ion exchange and amphoteric surface hydroxyl, groups which form inner sphere complex. With increasing pH, the surface charge becomes more negative [9,29–32] and, thereby, increasing the adsorption of metal ions.  $Cu^{2+}$  and  $Ni^{2+}$  adsorption to kaolin also occurs by ion exchange. The adsorption of cations to ion exchange sites is dominated by attractive electrostatic interactions.

Fitted Freundlich adsorption characteristics parameters ( $n$ ,  $K_F$ ) have been presented in Table 2, for Cu-kaolin, Cu-iron oxide, Ni-kaolin and Ni-iron oxide, respectively, at a pH of 4.5 and 11.5. It has also been shown that for all systems,  $K_F$ , which is a measure of the degree of affinity of the adsorbent for the adsorbates increases with increase in pH but there is a slight decrease in  $n$  with increase in pH for all systems. The effect of pH on  $K_F$  is less pronounced in case of metal-kaolin system than metal-iron oxide system. An explanation is offered in what follows.

The adsorption on kaolin occurs predominantly on the permanent negatively charged siloxanol sites and less on the variable-charged aluminol sites, which are strongly affected by the pH of the solution. Therefore, adsorption capacity  $K_F$  of kaolin does not increase by a large extent with increase in pH. Whereas, sorption occurs on variable (vis-à-vis fixed) charged surfaces for iron oxide and it is strongly pH dependent. Such dependency is reflected on the higher increase in  $K_F$  with pH Table 2. For Cu-kaolin system at pH 11.5, high value of adsorption capacity  $K_F$  Table 2 may be due to substantial changes of variable charged aluminol sites with the formation of inner

Table 2  
Freundlich Adsorption Characteristics Parameters,  $X = K_F C^n$

System	pH	$n$	$K_F$ ( $l\ g^{-1}$ )	Initial metal ion concentration
Cu-kaolin	4.5	1.11	0.65	10.4, 12.0, 16.3, 23.5 and 27.8 $mg\ l^{-1}$
	11.5	1.047	18.02	
Ni-kaolin	4.5	1.37	0.41	9.5, 12.4, 15.6, 18.8, 20.9 and 26.5 $mg\ l^{-1}$
	11.5	1.32	1.83	
Cu-iron oxide	4.5	0.21–0.70	7.94–23.44	9.4, 17.0, 19.8, 23.4 and 26.4 $mg\ l^{-1}$
	11.5	0.55	31.62	
Ni-iron oxide	4.5	0.60	4.75	11.4, 12.4, 16.9, 20.4 and 24.5 $mg\ l^{-1}$
	11.5	0.56	14.09	

sphere complexes on kaolin surface. The reason behind increase in adsorption capacity,  $K_F$  with increase in pH is mainly due to an increase in the number of negatively charged surface sites.

The other Freundlich empirical coefficient, ' $n$ ' is found to be less than one for metal-iron oxide system, whereas, for metal-kaolin system it is greater than unity at a fixed pH and small concentration range Table 2. Adsorption capacity of iron oxide is more with respect to kaolin but intensity of adsorption is less. This may be due to the fact that adsorption takes place mainly due to attractive van der Waals forces. Whereas, for kaolin system, adsorption intensity is high due to the presence of inherent negatively charged sites on the surface which are mainly utilized in adsorption by simply ion exchange process.

In both systems (particularly on iron oxide), adsorption is an interaction of adsorbing species with well-defined coordination sites (surface OH groups) to form surface-complex. A simple surface-complex model can reasonably explain such pH dependent adsorption mechanism, which is presented in elsewhere [33].

### 3.3.2. Comparison of adsorption equilibrium between metal-colloid and metal-sand systems

Fig. 7 presents the adsorption isotherms between metal kaolin and metal sand systems for a small concentration range. Here, for the sake of comparison adsorption density has been expressed as mg of adsorbate per unit specific area of adsorbent for both the systems. From these plots, one can observe that the amount of adsorption in case of Ni-kaolin as well as Cu-kaolin system is

higher than Ni-sand and Cu-sand system, implying that kaolin is a better adsorbent than sand.

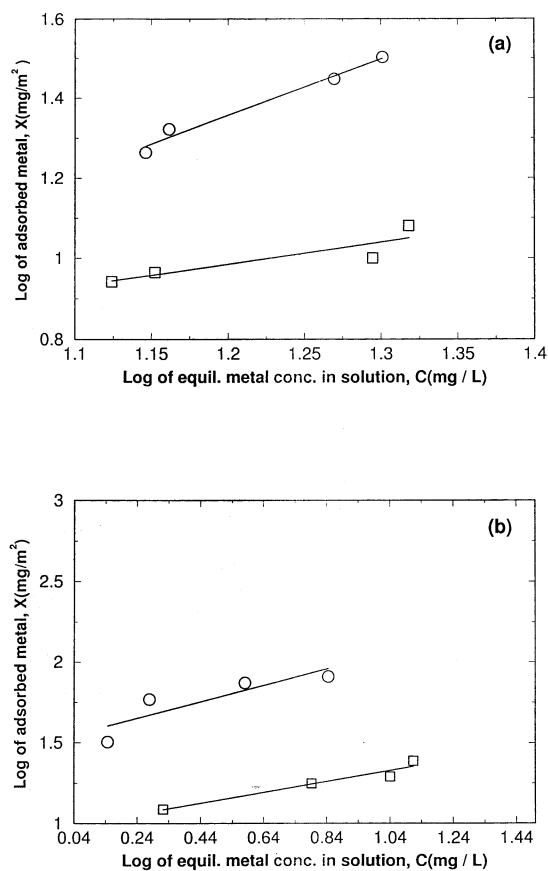


Fig. 7. Comparison on Freundlich adsorption isotherm. (a)  $\circ$  Ni-kaolin, pH, 4.5; ' $n$ ', 1.41; ' $K_F$ ', 0.456; Coeff., 0.99;  $\square$  Ni-sand system, pH, 4.5; ' $n$ ', 0.547; ' $K_F$ ', 2.12; Coeff., 0.88. (b)  $\circ$  Cu-kaolin, pH, 11.5; ' $n$ ', 0.50; ' $K_F$ ', 33.11; Coeff., 0.87;  $\square$  Cu-sand, ' $n$ ', 0.341; ' $K_F$ ', 9.33; Coeff., 0.97.

### 3.3.3. Application of batch adsorption parameter on breakthrough curves (BTCs) of $\text{Ni}^{2+}$ transport

In transport experiments, adsorption plays an important role on  $\text{Ni}^{2+}$  breakthrough patterns. Fig. 8 presents the measured as well as model predicted breakthrough curves (BTCs) based on batch adsorption data for three different beds. Breakthrough plots are presented as plots of  $C_c/C_{c0}$  against pore volumes (PV) where  $C_c$  is the aqueous phase effluent  $\text{Ni}^{2+}$  concentration, and  $C_{c0}$  is the influent  $\text{Ni}^{2+}$  concentration.

One observes from these BTCs that the breakthrough is delayed, as expected, as the content of kaolin in the bed is increased.  $\text{Ni}^{2+}$  eluted more slowly in the presence of colloidal kaolin than in its absence. Such delayed breakthrough is due to increased adsorption capacity of beds. Several reported models, which predict the transport of

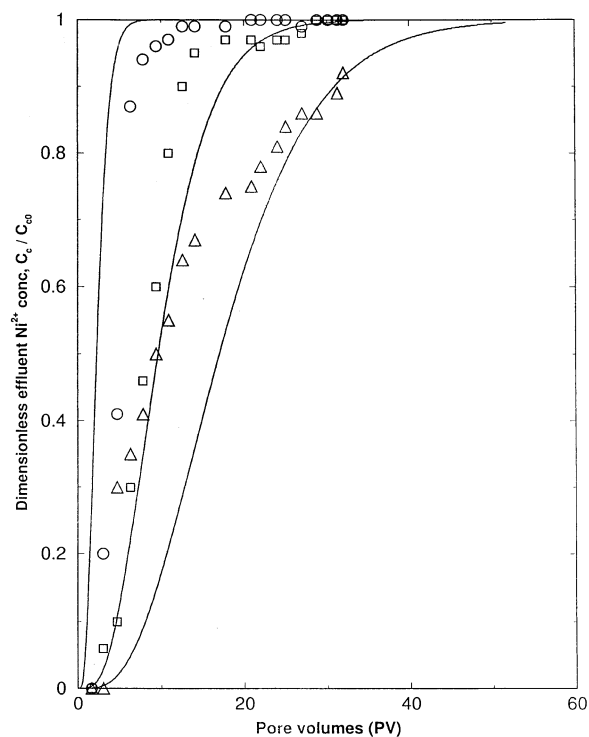


Fig. 8. Comparisons between  $\text{Ni}^{2+}$  BTCs from model prediction using batch data and measured BTCs during column flow experiments. — Batch based model, ○ Measured, Sand bed (0%), □ Measured, 2% bed and △ Measured, 4% bed.

inorganic contaminants in subsurface systems, have traditionally been based on a two-phase approach: the mobile fluid phase and the immobile solid phase. However, when colloidal particles are present in the system, the groundwater reservoir should be modified as a three phase porous media with two solid phases i.e. mobile colloidal fines and stationary matrix. Therefore, a three-phase equilibrium transport model has been developed which can successfully explain  $\text{Ni}^{2+}$  transport in presence of colloidal fines, kaolin. The model has been developed based on equilibrium adsorption of contaminants, hydrodynamic release, migration and capture of colloidal fines in groundwater flows. The model consists of mass balance equations for fine particles as well as for contaminants. Since the contaminant species reside in four different sites (mobile fines, captured fines, liquid and solid matrix), mass balance equations are written for each site. These equations with appropriate boundary conditions and initial conditions were numerically solved for a system of finite length. The details of the model development and validations are presented in elsewhere [5,33]. We have applied this model to find out BTCs for  $\text{Ni}^{2+}$  transport experiments. Three different beds are taken to typically represent this comparison. Only the composition of the bed i.e. weight percent of kaolin in the bed is different (0, 2, and 4%). Everything else remain the same for all column flow experiments i.e. superficial velocity of  $7.74 \times 10^{-5} \text{ m s}^{-1}$ , initial  $\text{Ni}^{2+}$  concentration of  $20.5 \text{ mg l}^{-1}$ , and a bed porosity of 0.32. The batch adsorption coefficient values for composite beds are calculated from the equation.

$K_m = K_s (1 - F) + F K_f$ , where  $K_s$  and  $K_f$  are the partition coefficients of sand and kaolin, respectively, obtained from fitted Freundlich equation with measured isotherm for which linear regression coefficient was above 90%, and  $F$  is the weight fraction of kaolin present in the bed.

One observes from this Figure that there are some disagreements between model calculations and the measurements. The disagreements between the model calculations and the measurements increase with the increase in kaolin content of the bed. The calculated BTCs using batch adsorption parameter values for sand–kaolin beds ap-

pear later as compared with measured BTCs. Such delay in breakthrough indicates that, the amount of adsorption in the bed is substantially lower than that could be predicted using batch adsorption measurements. Such disagreements are also indicated by the low percentage saturation (below 25%) of the bed [4,33]. Interestingly, the BTC for sand bed appear earlier than the measurements. This may indicate that the influence of external mass transfer in the adsorption process in the sand bed. From this comparisons study, we can conclude that parameter value based on batch adsorption studies, in general, over-predict the extent of adsorption and, hence, retardation of contaminant transport in column flow studies.

#### 4. Conclusions

- Batch adsorption studies show that contaminants such as  $\text{Ni}^{2+}$ ,  $\text{Cu}^{2+}$  adsorb more strongly on the naturally present colloidal fines, iron oxide and kaolin than on the solid matrix, sand material.
- The amount of cation adsorption increases with increase in pH but decreases with increase in adsorbent concentration.
- Freundlich adsorption equation reasonably describes the adsorption isotherms within this small concentration range. For Cu–iron oxide system at pH of 4.5, entire ranges of data is better fitted with two Freundlich equations with two different slopes, indicating the existence of two different sets of adsorption sites with different adsorption energy. Freundlich parameter, ' $K_F$ ' which is a measure of the adsorbent capacity is strongly dependent on system pH for metal–iron oxide system rather than metal–kaolin system. Whereas, other Freundlich parameter, ' $n$ ' which indicates the intensity of adsorption is less than one for metal–iron oxide but it is greater than one for metal–kaolin at fixed pH.
- Kaolin–sand beds retard the  $\text{Ni}^{2+}$  transport as compared with sand due to their higher adsorption capacity when there are no migration of kaolin particles. Parameter values based on batch adsorption studies, in general, over-pre-

dict the extent of adsorption as well as retardation in column flow measurements, indicating inapplicability of batch data on the prediction of colloid-associated contaminant transport in porous media.

#### Acknowledgements

One of the authors, Tushar Kanti Sen thanks Regional Engineering College, Rourkela-8 (Orissa), India, for allowing him to avail the study leave for his doctoral work under Quality Improvement Programme (QIP) scheme.

#### References

- [1] A.B. Kersting, D.W. Efurud, D.L. Finnegan, D.J. Rokop, D.K. Smith, J.L. Thompson, *Nature* 397 (1999) 56.
- [2] B.D. Honeyman, *Nature* 397 (1999) 23.
- [3] R. Kretzschmar, M. Borkovec, D. Grolimund, M. Elimelech, *Adv. in Agronomy* 199 (1999) 66.
- [4] T.K. Sen, S.P. Mahajan, and K.C. Khilar, *AIChE Jr.* (2002) (in press).
- [5] T.K. Sen, N. Nalwaya, and K.C. Khilar, *AIChE Jr.* (2002) (in press).
- [6] J.N. Ryan, M. Elimelech, *Colloid Surfaces A* 107 (1996) 1.
- [7] P. Trivedi, L. Axe, *Environ. Sci. Technol.* 34 (2000) 2215.
- [8] U.B. Neubauer, B. Nowalk, G. Furrer, R. Schulin, *Environ. Sci. Technol.* 34 (2000) 2749.
- [9] M.J. Angove, B.B. Johnson, J.D. Wells, *J. Colloid Interface Sci.* 204 (1998) 93.
- [10] R. Apark, K. Guclu, M.H. Turgut, *J. Colloid Interface Sci.* 203 (1998) 122.
- [11] L.E. Katz, K.F. Hayes, *J. Colloid Interface. Sci.* 170 (1995) 477.
- [12] K.C. Swallow, D.N. Hume, M. Francois, M. Morel, *Environ. Sci. Technol.* 14 (1980) 1327.
- [13] M.M. Benjamin, J. Leckie, *J. Colloid Interfac. Sci.* 79 (1981) 209.
- [14] Jr. W. Walter J, M.M. Paul, K.E. Lynn, *Water Res.* 25 (1991) 449.
- [15] K. Subramaniam, S. Yiacoumi, T. Costars, *Colloids and Surfaces A* 177 (2001) 133.
- [16] E. Gorden, Jr, V.E. Brow, W.H. Henrich, L.D. Casey, C. Clark, A. Eggleston, D. Felmy, W. Goodman, M. Gratzel, M.I. McCarthy, K.H. Nealson, D.A. Sverjensky, M.F. Toney, J.M. Zachara, *Chem. Rev.* 99 (1999) 77.
- [17] D.W. Fuerstenau, K.J. Osseo-asare, *Colloid Interface Sci.* 118 (1987) 525.
- [18] D.A. Dzombak, F.M.M. Morel, *J. Colloid Interface Sci.* 112 (1986) 589.

- [19] R.M. Cornell, U. Schwertmann, *The Iron Oxide-Structures, Properties, Reactions Occurrence and Uses*, VCH, New York, 1998.
- [20] P. Johnson, R.N. Sun, M. Elimelech, *Environ. Sci. Technol.* 30 (1996) 3284.
- [21] K.F. Hayes, J.O. Leckie, *J. Colloid Interface Sci.* 115 (1987) 565.
- [22] S.A. Hussain, S. Demirci, G. Ozbayoglu, *J. Colloid Interface Sci.* 184 (1996) 535.
- [23] D.J. O'Conner, J.P. Connelly, *Water Res.* 14 (1980) 1517.
- [24] R.L. Curl, G.A. Keolun, *Environ. Sci. Technol.* 18 (1984) 916.
- [25] G. Pan, P.S. Liss, *J. Colloid Interface Sci.* 201 (1998) 71.
- [26] T.C. Voice, W.J. Weber, *Environ. Sci. Technol.* 19 (1985) 789.
- [27] T.C. Voice, C.P. Rice, W.J. Weber, *Environ. Sci. Technol.* 17 (1983) 513.
- [28] J.P. Mckinley, E.A. Jenne, *Environ. Sci. Technol.* 25 (1991) 2082.
- [29] W.R. Puls, R.M. Powell, *Environ. Sci. Technol.* 26 (1992) 614.
- [30] K.C. Khilar, H.S. Fogler, *Migration of Fines in Porous Media*, Kluwer Academic Publisher, Dordrecht, Boston and London, 1998.
- [31] S.F. Kia, H.S. Fogler, M.G. Reed, *J. Colloid Interface Sci.* 118 (1987) 158.
- [32] D.J.A. Williams, K.P. Williams, *J. Colloid Interface Sci.* 65 (1) (1978) 79.
- [33] T.K. Sen, "Studies on colloidal fines-associated contaminant transport in porous media", Ph.D thesis, Department of Chemical Engineering, I.I.T Bombay, Mumbai India (2001).